Available online at www.sciencedirect.com
SCIENCE DIRECT
Polymer 47 (2006) 4824–4830
polymer
www.elsevier.com/locate/polymer

Effect of loading-rate on fracture micromechanism of methylmethacrylate–butadiene–styrene polymer blend

M. Todo [a,*], J. Takahashi [b,c], H. Watanabe [c], J. Nakamoto [c], K. Arakawa [a]

[a] Research Institute for Applied Mechanics, Kyushu University, 6-1 Kasuga-koen, Kasuga, Fukuoka 816-8580, Japan
[b] Interdisciplinary Graduate School of Engineering Science, Kyushu University, Kasuga, Fukuoka 816-8580, Japan
[c] Polymer Research Center, Denki Kagaku Kogyo Kabushiki Kaisha, Ichihara, Chiba 290-8588, Japan

Received 31 January 2006; received in revised form 22 April 2006; accepted 24 April 2006
Available online 15 May 2006

Abstract

Methylmethacrylate–butadiene–styrene (MBS) polymer blends having two different types of rubber particle distribution, monomodal and bimodal, were prepared, and their fracture properties and fracture mechanisms were investigated under quasi-static and impact loading. A fracture property, maximum J-integral J_{max}, was evaluated at both loading-rates, and it was shown that J_{max} values of the bimodal MBSs are much greater than that of the monomodal with small particles, and slightly better than that of the monomodal with large particles. Thick damage zones were observed in the crack-tip regions in the bimodal and monomodal with large particles, indicating larger energy dissipation during fracture initiation than in the monomodal with small particles in which damage zone is much thinner. TEM micrographs exhibit that extensive plastic deformation under quasi-static rate and multiple craze formation under impact loading rate are the primary toughening mechanisms in the bimodal MBS blends. By assessing both fracture properties and transparency, the bimodal blend with blend ratio: 2.5/7.5 (=140 nm/2.35 μm; total rubber particle content is 10 wt%) was proved to show the best performance as MBS polymer blend with satisfiable transparency and high fracture resistance.

Keywords: Polymer blend; Bimodal distribution; Impact fracture resistance

1. Introduction

Methylmethacrylate–styrene (MS) resin has widely been used in many industrial fields mainly owing to its transparency. As application of MS resin is getting wider, requirement for its mechanical properties also becomes higher. Especially, improvement of impact resistance is one of the main concerns since MS exhibits brittle fracture behavior at service temperatures. Therefore, methylmethacrylate–butadiene–styrene (MBS) blend, a rubber toughened MS resin, has been developed to increase the fracture resistance of MS, and has exhibited an excellent ability for impact energy absorption [1–3]. However, the detail of fracture mechanism has not been clarified yet, and optimization of particle conditions such as size and content is still one of the most important unknown factors for material design.

Effectiveness of rubber modification on the toughening of brittle thermoplastic polymers has widely been investigated, and the toughening mechanisms have been reported for some rubber-toughened polymers such as HIPS, ABS and rubber-toughened PMMA (RT-PMMA). From structural point of view, bimodal distribution of rubber particles in HIPS is known to be effective on improvement of impact resistance [4], where 'bimodal' means large and small rubber particles are distributed in the matrix polymer. It is also noted that in general, thermoplastic polymers exhibit clear dependence of loading-rate on the fracture properties [5,6]. For example, it was shown that the fracture toughness of a RT-PMMA suddenly drops at impact loading-rate, and the toughness value becomes almost equivalent to that of neat PMMA. Thus, it is crucial to characterize the rate-dependency on the fracture properties and mechanisms of such rubber-toughened polymers.

In the present study, MBS resins with monomodal and bimodal particle distribution were synthesized to study the effects of particle size and distribution pattern on fracture properties and mechanisms under static and impact loading. Maximum J-integral values were measured at both loading-rates, and fracture mechanisms were also examined using an polarizing optical microscope (POM) and transmission electron microscope (TEM).

* Corresponding author. Tel.: +81 92 583 7762; fax: +81 92 583 7763.
E-mail address: tohdoh@riam.kyushu-u.ac.jp (M. Todo).

0032-3861/$ - see front matter © 2006 Elsevier Ltd. All rights reserved.
doi:10.1016/j.polymer.2006.04.042

2. Experimental

2.1. Material and specimen

Two different types of MBS resins, monomodal and bimodal types, were prepared to investigate the effect of rubber particles on the fracture property and fracture mechanism. behavior The 'monomodal' type contains one size of rubber particles. Two kinds of butadiene rubber particles having different diameter sizes, 140 nm and 2.35 μm, were prepared for this type of MBS resin. The 'bimodal' type contains both the particles, thus bimodal distribution of particles is achieved. The total weight fraction of the particles was fixed at 10 wt% for both types. For the bimodal MBS resins, the ratio of the two particles, 140 nm/2.35 μm, were chosen to be 2.5/7.5, 5/5 and 7.5/2.5. Thus, two monomodal and three bimodal MBS resins were prepared as pellets.

Procedure of material processing of these pellets is as follows. MBS resins were prepared by polymerizing a solution containing 10 wt% of styrene–butadiene copolymer (styrene/butadiene =4/6), 50 wt% of styrene, 35 wt% of methyl methacrylate and 5 wt% of *n*-butyl acrylate. Bulk-suspension polymerization was applied in this process. Two kinds of MBS resins having the small and large particles, respectively, were prepared by changing stirring speed in the bulk polymerization. After the bulk-suspension polymerization, the products in the form of beads were processed into pellets by a single screw extruder at a cylinder temperature of 220 °C.

Microstructures of the MBS resins were observed using a transmission electron microscope (TEM). Bulk samples of the MBS resins were stained with osmic acid and then, sliced into ultrathin sections using a ultra-microtome. The microstructures of the two monomodal and a bimodal are shown in Fig. 1. Rubber particles are seen to be distributed homogeneously. The structure of the large particles is recognized as salami-structure that is usually formed by bulk polymerization.

Plates of 5 mm thick were then fabricated from the pellets using a hot press. Single-edge-notch-bend (SENB) specimens were then made from these plates to measure fracture property. The geometry of the specimen is shown in Fig. 2(a).

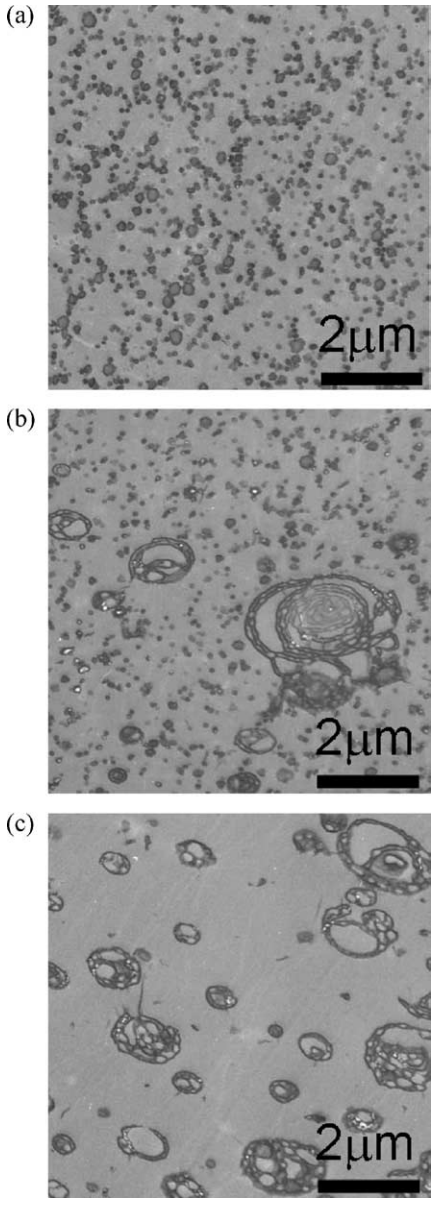

Fig. 1. TEM micrographs of microstructures of three types of MBS resins. (a) Monomodal (140 nm: 10 wt%). (b) Bimodal (140 nm: 7.5 wt%, 2.35 μm: 2.5 wt%). (c) Monomodal (2.35 μm: 10 wt%).

2.2. Mode I fracture test

Three-point bending tests of the SENB specimens prepared were performed at a quasi-static loading rate of 1 mm/min using a servohydraulic testing machine. Load-time and displacement-time relations were recorded using a digital recorder. Mode I fracture tests were also performed at an impact loading rate of 1.3 m/s using an drop weight type impact testing machine attached with a dynamic displacement measuring system [7,8]. A schematic diagram of the impact testing system is shown in Fig. 3. Load was measured using the piezoelectric load cell, and load-point displacement was measured using the displacement measuring system where an optical fiber was stick at the load-point of the specimens, and laser beam coming through the fiber was detected by the position sensing detector.

Since, nonlinear mechanical behavior was observed on the load–displacement curves obtained from the mode I fracture tests, *J*-integral, a nonlinear fracture mechanics parameter that can be regarded as an energy release rate, was used as a fracture property [9,10]. The maximum *J*-integral, J_{Imax}, was evaluated from the load–displacement data using the following formula

$$J_{\mathrm{Imax}} = \frac{\eta U_{\max}}{B(W-a)} \tag{1}$$

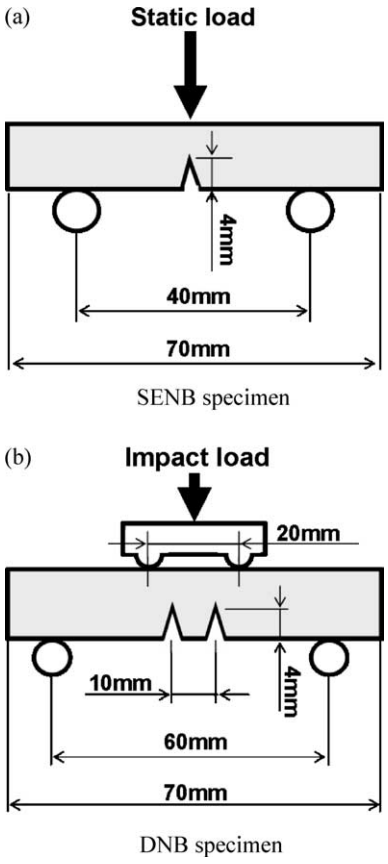

Fig. 2. Geometries of SENB and DNB specimens. (a) SENB specimen. (b) DNB specimen.

where U_{max} is the energy expressed as the area under the load–displacement curve up to the maximum load. B, W and a are the thickness, the width and the initial crack length of the specimen, respectively. η is a geometrical correction factor, which is equal to 2 for standard SENB specimen.

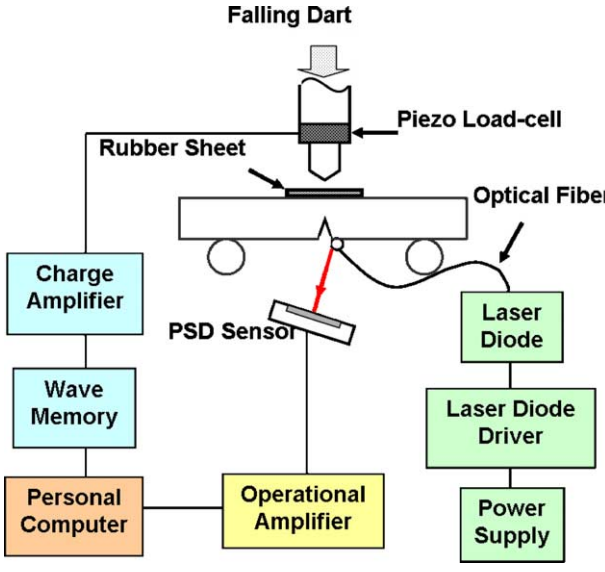

Fig. 3. Schematic diagram of impact testing system.

2.3. Transparency measurement

Transparency is one of the most important factors for MS resin for industrial use, and therefore, improvement of impact resistance by rubber toughening has to be achieved without sacrifice of transparency. Haze values of the MBS resins were evaluated as a measure of transparency. The plates (120 mm × 40 mm) of 2 mm thickness were used for the samples for haze measurements. Higher haze implies lower transparency.

2.4. Microscopy of damage zone and fracture surface

Crack-tip regions of the specimens with arrested cracks were observed using a polarizing optical microscope (POM) to understand the shape and size of damage zones developed under high stress state in the crack-tip regions. For quasi-static loading condition, SENB specimens were used to create arrested cracks accompanied by damage zones formed in the notch-tip regions by unloading the specimens at the maximum load. For impact loading condition, double-notch-bend (DNB) specimens were used to obtain damage zones in the notch-tip regions [11]. The geometry of DNB specimen is shown in Fig. 2(b). If four-point impact bend test of s DNB specimen is performed, then a short arrested crack with damage zone is possibly created from one of the notch-tips. A crack initiated from the other notch-tip propagates through the specimen width and fractures the specimen completely. Thin samples were prepared from the notch-tip regions of the SENB and DNB specimens by using thin sectioning technique, and then observed using POM.

Microdamages generated within the damage zones were also observed using a transmission electron microscope (TEM) to characterize the micromechanisms of fracture. Ultra-thin sections were prepared from the damage zones stained with osmic acid using ultra-microtome.

3. Results and discussion

3.1. Fracture properties

Load–displacement curves are shown in Fig. 4. It is clearly seen that the monomodal with small particles exhibits relatively brittle behavior compared to the other two resins. It is thus presumed that the large particles enhance the ductility of MBS blend. The slope of the load–displacement curve of the monomodal with small particles is the largest and the monomodal with large particles smallest. This indicates that stiffness reduction is caused by the large particles more than the small particles.

The static and impact J_{Imax} values are shown as a function of large particle content in Fig. 5(a) and (b), respectively. J_{Imax} values of MS resin are also shown in these figures. It is obvious that the static values of MBS are much higher than that of MS. It is also seen that the static value is maximized with blend ratio, 7.5/2.5 (=140 nm/2.35 μm). It should be noted that all three kinds of bimodal MBSs exhibited higher J_{Imax} values than the two monomodal resins, suggesting that bimodal

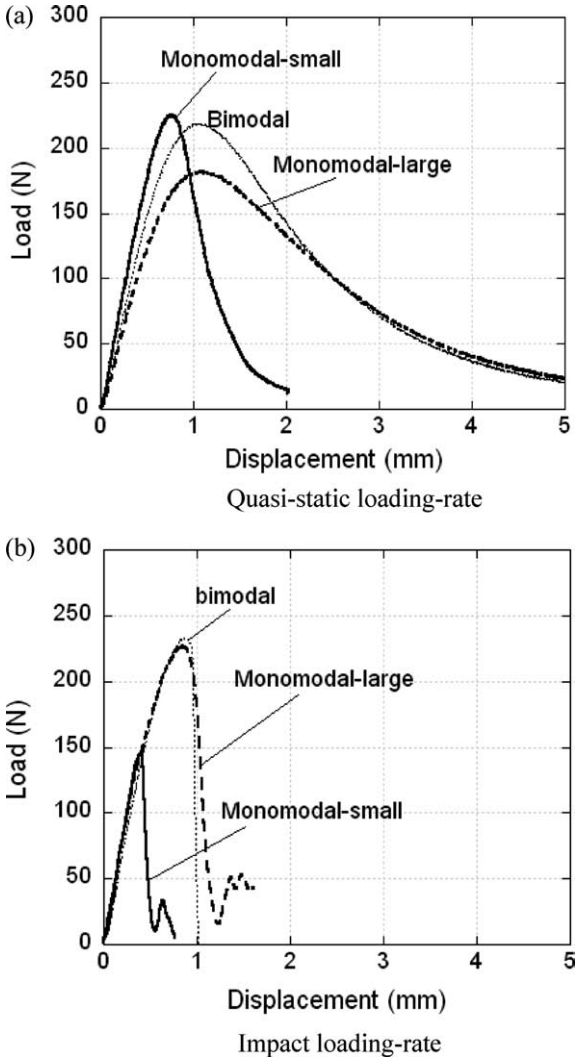

Fig. 4. Load–displacement curves at quasi-static and impact loading-rates.

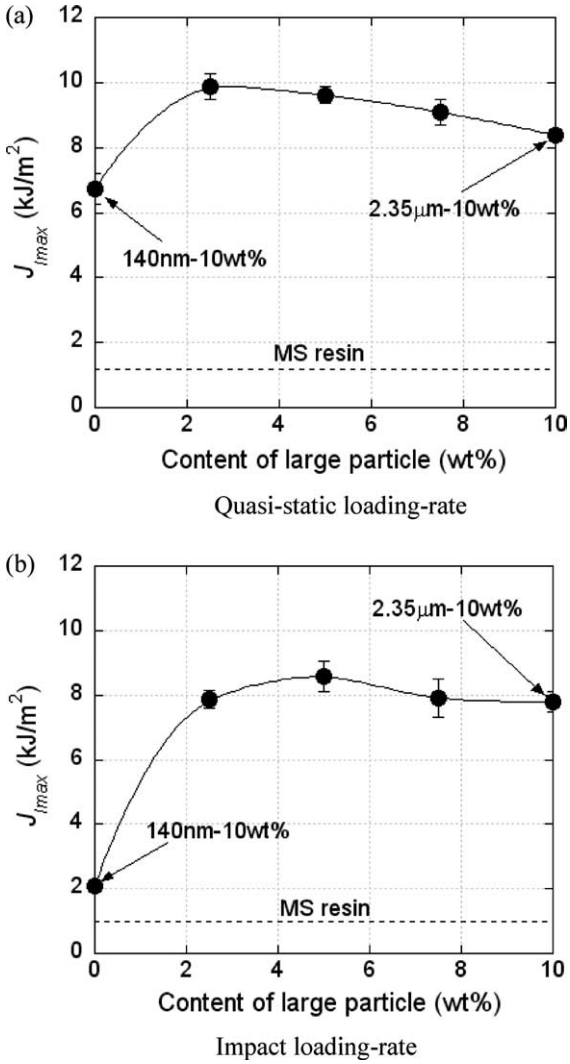

Fig. 5. Effect of large particle content on the maximum J-integral, J_{Imax}. (a) Quasi-static loading-rate. (b) Impact loading-rate.

distribution is effectively improved the static fracture property. Fig. 5(b) shows that the impact values of the three bimodal MBSs and the monomodal MBS with 2.35 μm particles are much higher than that of MS, while the impact value of the monomodal MBS with 140 nm particles is very close to that of MS. It is thus concluded that the large particle (2.35 μm diameter) is much more effective on the impact resistance of monomodal MBS than the small particle (140 nm diameter). The impact values of the bimodal MBSs are slightly better than the monomodal MBS with large particles, and the impact value is maximized with blend ration, 5/5 (=140 nm/2.35 μm).

3.2. Transparency

Haze values are shown as a function of large particle content in Fig. 6. Smaller haze value indicates better transparency. The transparency of the monomodal MBS with small particles is about the same as that of MS resin. The transparency becomes worse with increase of large particle content. In general, polymers with haze values less than 5% is recognized as transparent materials; therefore, in the present study, only the bimodal MBS with blend ratio, 7.5/2.5 (=140 nm/2.35 μm), can be regarded as a transparent polymer.

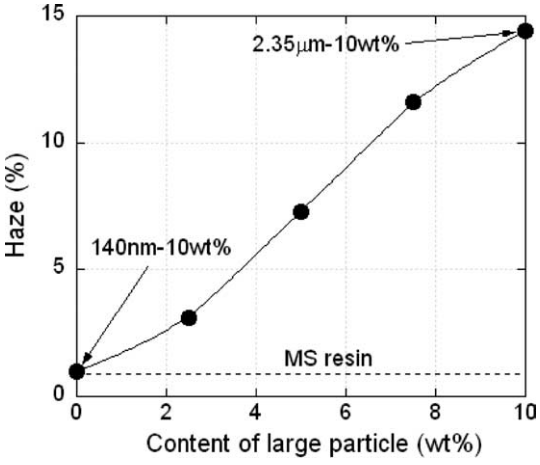

Fig. 6. Effect of large particle content on transparency index, haze.

3.3. Characterization of fracture micromechanism

POM micrographs of damage zones observed under quasi-static loading in the two monomodal MBSs, denoted as small (140 nm diameter) and large (2.35 μm diameter), and a bimodal MBS with the blend ratio: 5/5, are shown in Fig. 7. J_{Imax} values are also shown in the parentheses. It is seen that the damage zone of the large is very similar to the bimodal with thick damages, while the damage zone of the small is thinner than the other two MBSs. It is noted that such thick damage zones correspond to higher J_{Imax} values since in general, larger amount of damages dissipate more energy during crack initiation process. POM micrographs of damage zones under impact loading are shown in Fig. 8. These impact damage zones are much different from the static ones. The impact damage zone of the small is much smaller than those of the other MBSs, corresponding to the low J_{Imax} value. The size of the damage zone of the bimodal is slightly larger than that of the large, suggesting that the fracture energy dissipation in the bimodal is also slightly greater than that of the large, which exactly coincides with the superiority of J_{Imax} as shown in the figure.

TEM micrographs of crack-tip micro-damage formations within the damage zones under static loading are shown in Fig. 9. For the small, rows of cavitated rubber particles accompanied by shear yielding are observed, and these microdamages appear to grow in the direction almost parallel to the crack growth direction. For the bimodal, cavitations of both small and large particles and larger scall plastic deformation of the particles and the surrounding matrix are observed, indicating that greater amount of energy is dissipated in the crack-tip region than in the small. For the large, crazes (indicated by the black arrows) and plastic deformation of particles and matrix are observed. Multiple crazes are seen to be generated from a single particle. It is known that crazes are initiated from some points along the circumference of salami-structure rubber particle [12]. This is thought to be mainly due to multiple stress concentration in salami-structure where polymer phases are distributed within rubber phase.

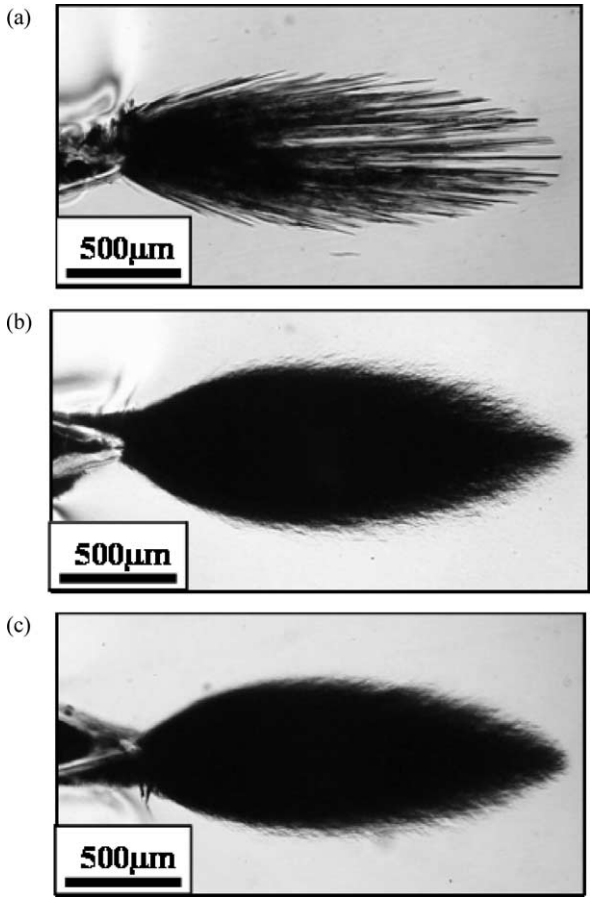

Fig. 7. Damage zone formation in notch-tip region under quasi-static loading. (a) Small (6.74 kJ/m^2). (b) Bimodal (9.61 kJ/m^2). (c) Large (8.38 kJ/m^2).

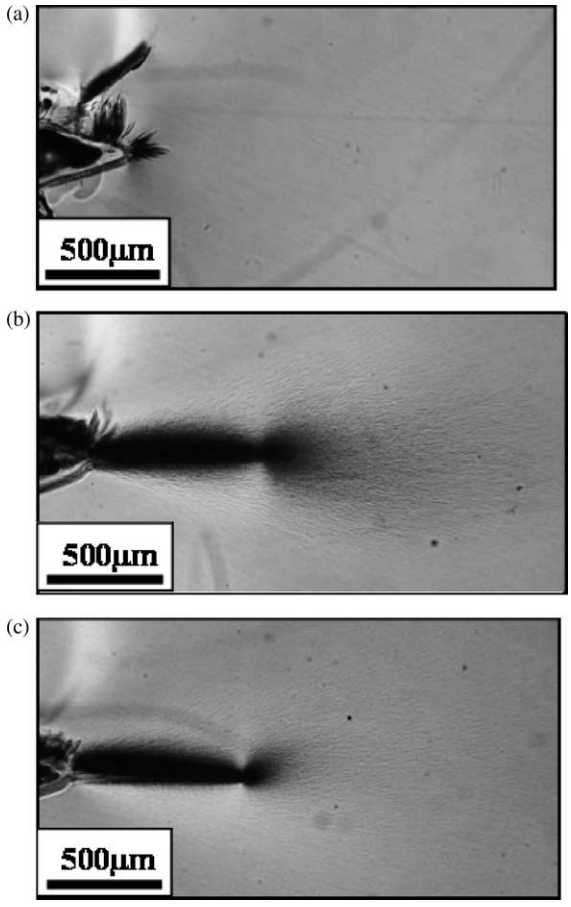

Fig. 8. Damage zone formation in notch-tip region under impact loading. (a) Small (6.74 kJ/m^2). (b) Bimodal (9.61 kJ/m^2). (c) Large (8.38 kJ/m^2).

In general, localized shear yielding is known to be the primary energy dissipation mechanism in rubber toughened thermoplastics [13], and in the present MBS resins, the bimodal exhibiting the most extensive plastic deformation possesses the highest J_{Imax} value. It is thus concluded that under quasi-static loading, the bimodal distribution tends to extend shear yielding region, and therefore, improves the fracture resistance. Cavitation of a rubber particle is thought to release the internal residual stress within the particle, and therefore, intensifies local stress concentration in the surrounding matrix [14]. In the

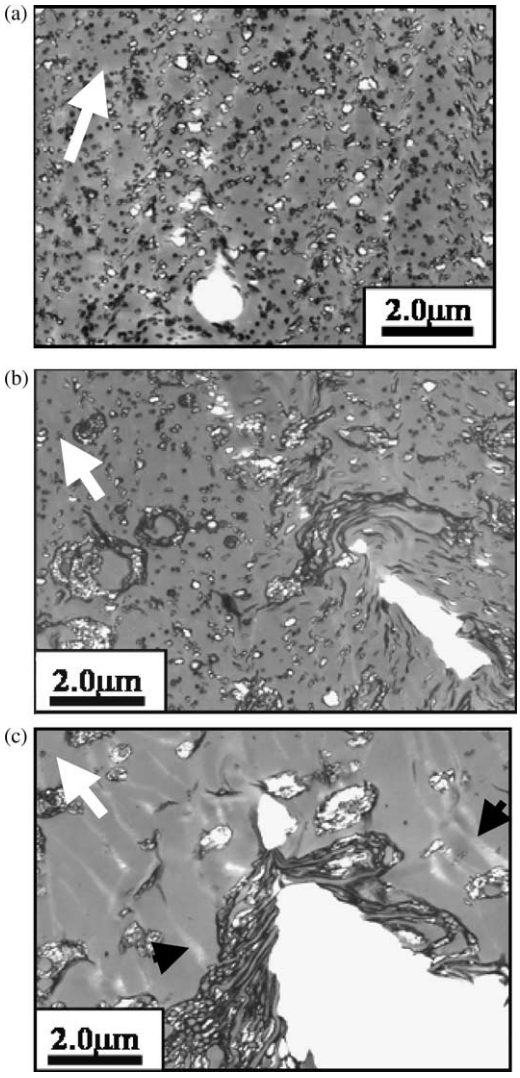

Fig. 9. Microdamage formations within damage zones under quasi-static loading. The white arrows indicate the direction of crack propagation. (a) Small (6.74 kJ/m^2). (b) Bimodal (9.61 kJ/m^2). (c) Large (8.38 kJ/m^2).

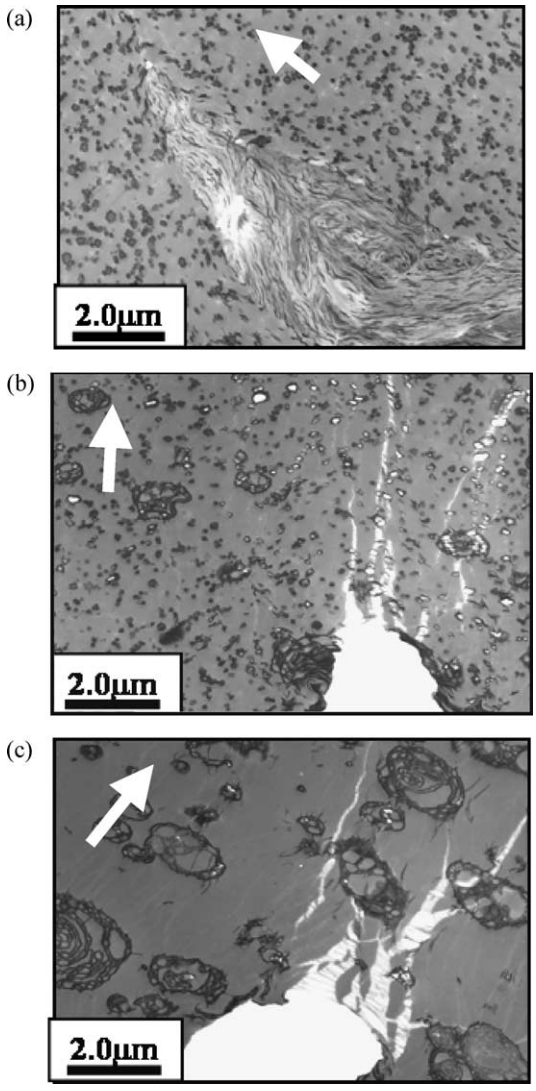

Fig. 10. Microdamage formations within damage zones under impact loading. The white arrows indicate the direction of crack propagation. (a) Small (6.74 kJ/m^2). (b) Bimodal (9.61 kJ/m^2). (c) Large (8.38 kJ/m^2).

bimodal, cavitations are generated in both small and large particles, and hence the region involving cavitated particles are larger than the monomodal resins.

TEM micrographs of crack-tip microdamage formations under impact loading are shown in Fig. 10. A unique plastic deformation is formed in the restricted region in the vicinity of the crack-tip in the small. This kind of localized deformation appears to be generated by viscosity flow due to heat generation under high strain-rate condition, that is typical in thermoplastic polymers [15–18]. On the other hand, the bimodal shows multiple crazes originated from the crack-tip. This kind of microcraze formation is usually seen in rubber toughened thermoplastic polymers [19–23]. Each craze grows as connecting rubber particles. Cavitations of rubber particles are also observed in this MBS resin. The large also exhibits similar craze formation with less number of particle cavitations. Thus, propagating longer crazes with particle cavitations in the bimodal result in higher energy dissipation, and therefore, higher J_{Imax} than in the monomodal MBSs. Heat generation in the crack-tip region of the small MBS causes softening of the local region, and therefore, tends to reduce the impact fracture resistance, i.e. much lower J_{Imax} value. On the contrary, in the bimodal and the large MBSs, most of impact energy is thought to be absorbed mainly through deformation of large particles, and hence, heat generation in the crack-tip region is suppressed.

4. Conclusions

Fracture properties and fracture micromechanisms of MBS polymer blends with monomodal and bimodal distribution of rubber particles were investigated under quasi-static and impact loading to assess the effect of type of particle distribution on the toughening behavior. Results were obtained as follows:

(1) Nonlinear fracture property, J_{Imax}, of bimodal MBSs is higher than monomodal MBSs under both loading conditions. For quasi-static loading-rate, the bimodal MBS with blend ratio 2.5/7.5 (= 140 nm/2.35 μm) shows the highest J_{Imax} value, and for impact loading-rate, the blend ratio 5/5 exhibits the highest value. Introducing the evaluation index, which includes both transparency and impact resistance, the blend ratio 2.5/7.5 shows the best performance at impact rate. Thus, the bimodal MBS with the blend ratio 2.5/7.5 is regarded as an optimized system in MBS polymer blends.

(2) The primary toughening mechanisms in bimodal MBS are extensive plastic deformation of rubber particles and the surrounding matrix in the crack-tip region with particle cavitations under quasi-static loading, and multiple crazes initiated from crack-tip and propagated as connecting cavitations under impact loading.

References

[1] Takahashi J, Nakamoto J, Ito T. Kobunshi Rombunshu 2002;59(9):527.
[2] Takahashi J, Nakamoto J, Ito T. Kobunshi Rombunshu 2003;60(1):6.
[3] Takahashi J, Watanabe H, Nakamoto J. Kobunshi Rombunshu 2004; 61(2):114.
[4] Okamoto Y, Miyagi H, Kakugo M. Macromolecures 1991;24:5639.
[5] Todo M, Shinohara N, Arakawa K. J Mater Sci Lett 2002;21:1203.
[6] Park SD, Todo M, Arakawa K. J Mater Sci 2004;39:1113.
[7] Todo M, Nakamura T, Takahashi K. J Renif Plast Compos 1999; 18(15):1415.
[8] Todo M, Nakamura T, Takahashi K. J Compos Mater 2000;34(8):630.
[9] Lu ML, Chang FC. Polymer 1995;36(13):2541.
[10] Lu ML, Chiou KC, Chang FC. Polymer 1996;37(19):4289.
[11] Sue HJ. Polym Eng Sci 1991;31(4):270.
[12] Dillon M. J Mater Sci 1982;17:1903.
[13] Takaki A, Hasegawa T, Isogawa M, Narisawa I. Polym Eng Sci 1994; 34(8):680.
[14] Jar PYB, Todo M, Takahashi K, Konishi K, Shinmura T. Plast Rubber Compos 2001;30(3):101.
[15] Williams JG. Inter J Fract Mech 1972;8(4):393.
[16] Doll W. Eng Fract Mech 1973;5:259.
[17] Tomashevskii EE, Egorov EA, Savostin AY. Inter J Fract 1975;11(5):817.
[18] Fuller KNG, Fox PG, Field JE. Proc R Soc London 1975;A-341:537.
[19] Seward RJ. J Appl Polym Sci 1970;14:852.
[20] Beahan P, Thomas A, Bevis M. J Mater Sci 1976;11:1207.
[21] Keskkula H, Schwarz M, Paul DR. Polymer 1986;27:211.
[22] Michler GH. Polymer 1986;27:323.
[23] Todo M, Takahashi K, Jar PYB, Beguelin Ph. JSME Iner J 1999; 42(4):585.